

Decay of MHD-Scale Kelvin-Helmholtz Vortices Mediated by Parasitic Electron Dynamics

T. K. M. Nakamura, D. Hayashi, and M. Fujimoto

Department of Earth and Planetary Sciences, Tokyo Institute of Technology, 2-12-1 Ookayama, Meguro, Tokyo 152-8551, Japan

I. Shinohara

Japan Aerospace Exploration Agency/Institute of Space and Astronautical Science,

3-1-1 Yoshino-dai, Sagami-hara, Kanagawa 229-8510, Japan

(Received 24 April 2003; published 9 April 2004)

We have simulated nonlinear development of MHD-scale Kelvin-Helmholtz (KH) vortices by a two-dimensional two-fluid system including finite electron inertial effects. In the presence of moderate density jump across a shear layer, in striking contrast to MHD results, MHD KH vortices are found to decay by the time one eddy turnover is completed. The decay is mediated by smaller vortices that appear within the parent vortex and stays effective even when the shear layer width is made larger. It is shown that the smaller vortices are basically of MHD nature while the seeding for these is achieved by the electron inertial effect. Application of the results to the magnetotail boundary layer is discussed.

DOI: 10.1103/PhysRevLett.92.145001

PACS numbers: 52.35.Py, 52.35.Qz, 52.65.Kj, 94.30.Di

The Kelvin-Helmholtz instability (KHI) is a well-known hydrodynamic instability that grows in a velocity shear layer, which is studied well also in the magneto-hydrodynamics (MHD) [1–3]. When the magnetic field is perpendicular to the flow, which is the geometry we will concentrate on hereafter, the magnetic field tends to two dimensionalize the dynamics onto the plane perpendicular to the magnetic field. This is in contrast to ordinary hydrodynamic situations in which three-dimensional effects are crucial [4,5].

MHD equations are derived by assuming that the dynamics at smaller scales (ion and electron scales) do not crucially affect the dynamics at MHD scales. While the equations seem to describe large scale dynamics of plasmas well, recent studies have shown that coupling to ion/electron scales can be essential in dynamic MHD-scale phenomena such as reconnection [6–9]. In this Letter, we show that MHD-scale KHI is another example of this category.

The magnetotail boundary layer separates the tenuous stagnant magnetospheric plasma from the dense shocked-solar wind and, thus, is a shear layer as well as a current layer whose width is several times the ion inertial length [10]. Since the ion scales are not negligible, ion effects might be crucial for the dynamics therein. We have found that, for the perpendicular geometry, behavior of KHI in Hall-MHD (two-fluid system with ion inertial effects taken into account) is found to be essentially the same as in MHD, implying that the ion inertial effects are not crucial. When ion finite Larmor radius effects are taken into account, if the density is uniform across the shear layer, large scale ion mixing, which does not take place in MHD, was shown to occur [11]. This process, which has been suggested to be the cause of the large scale mixing observed in the magnetotail boundary layer [12–14], however, becomes inefficient with moderate density

jump across the shear layer [15] and its relevance to the magnetotail issue is questionable.

Electron effects on KHI have been addressed thus far by full particle simulations [16], however, various artifacts, such as small ion-to-electron mass ratio, have prevented us from reaching definitive conclusions. We show that MHD-scale vortices quickly decay by coupling to electron inertial effects. Interestingly, the decay proceeds equally vigorously even when the vortex size is relatively large and is expected in the magnetotail boundary layer.

The simulations are done by two-dimensional two-fluid equations including finite electron inertia. Assuming charge neutrality, the equations are the same as the MHD equations

$$\frac{\partial n}{\partial t} + \nabla \cdot (n \mathbf{V}_i) = 0, \quad n \frac{d\mathbf{V}_i}{dt} = -\nabla P + \mathbf{J} \times \mathbf{B},$$

$$\frac{d}{dt} \left(\frac{P}{n^\gamma} \right) = 0,$$

except that the magnetic field \mathbf{B} is time advanced by [17]

$$\frac{\partial}{\partial t} \left(1 - \frac{1}{M} \Delta \right) \mathbf{B} = \nabla \times \left[\mathbf{V}_e \times \left(1 - \frac{1}{M} \Delta \right) \mathbf{B} \right],$$

where \mathbf{V}_e is the electron bulk flow, n is the number density, and M is the ion-to-electron mass ratio. \mathbf{V}_e is calculated by $\mathbf{V}_i - \mathbf{J}/n$, where \mathbf{V}_i is the ion bulk flow and $\mathbf{J} = \nabla \times \mathbf{B}$ is the current density. Note that the normalizations are made as follows: the magnetic field \mathbf{B} and the density n by the characteristic values B_0 and n_0 , respectively; the velocities, time, and length by the Alfvén velocity V_{A0} based on B_0 and n_0 , inverse of the ion gyrofrequency Ω_{i0} based on B_0 , and the ion inertial length $\lambda_{i0} = V_{A0}/\Omega_{i0}$, respectively. The characteristic electron inertial length is given by $\lambda_{e0} = \sqrt{1/M}$ (the term $\frac{1}{M} \Delta$ in the induction equation implies $\lambda_{e0}^2 \Delta$).

The system is periodic in the flow (x) direction with its size equal to the wavelength of the fastest growing KH mode $L_x = 15D$ [18], where D denotes the half thickness of the shear layer. Conducting walls are located at $y = \pm 10D$. The initial conditions are given as follows: $V_{ix}(y) = V_0 \tanh(y/D)$; $n(y) = 1 + (R - 1) \times \{1 + \tanh(y/D)\}/2$. R (> 1) is the density ratio across the shear layer. With the magnetospheric situation in mind, the higher (lower) density side $y > 0$ ($y < 0$) is called the magnetosheath (magnetosphere). The ion temperature is assumed to be uniform and the electron temperature is set to zero for simplicity. The magnetic field is perpendicular to the plane of the calculation and is positive in the z direction. The magnetic field intensity changes across the shear layer to maintain the total pressure balance. $n(y)\beta_0 + B_z(y)^2 = \text{const}$; β_0 is the plasma beta in the magnetosphere. That is, the velocity shear layer is set to be a current layer as well, just like the magnetotail boundary layer. When $V_0 < 0$, the sense of the velocity shear $[\nabla \times \mathbf{V}_i] \cdot \mathbf{B} > 0$ corresponds to the duskside tail boundary. We choose $V_0 = \pm 0.5$ and $R = 2.5$. Setting $\beta_0 = 0.5$, $B_z(y)$ varies from 1 (magnetosphere) to 0.5 (magnetosheath).

Flow perturbation $\delta V_{iy} = 0.05 \exp[-(y/D)^2] \times \sin(2\pi x/L_x)$ as well as small amplitude (10^{-3}) random perturbations in the magnetic field are added initially. Since the basic dynamics are of hydrodynamic nature, we introduce the time unit $D = D/V_{A0}$ in presenting the results (e.g., $T = 50D$), which makes the comparison among results from different D cases easier.

The numerical schemes are the fourth-order finite difference in space and the fourth-order Runge-Kutta in time, with fourth-order hyperviscosity added to ensure numerical stability. The size of the spatial grid is $\frac{1}{2} \lambda_{e0}$. The results are tested by changing the hyperviscosity magnitude, by performing a run with the fifth-order upwind scheme, and by reducing the grid size to half.

The magnetic induction equation is derived by assuming that the ion density and the ion velocity do not vary substantially over the electron inertial scale. Furthermore, the two $\frac{1}{M}$ factors should be $\frac{1}{M_n}$, to be precise. This approximation is adopted to save the computational time. Runs with the precise equation for the cases of $R = 2.5, 4$, and 8 have confirmed the essential results to be unchanged by this simplification, at least for the range of the density ratio we are interested in. This sets a firm basis for us to discuss the magnetotail situation using the present results. Another confirmation of the results is done by running another two-fluid code that is built according to a different formulation [19], from which we have obtained essentially identical results.

Figure 1 shows the time sequence of density (left) and current density $[(J_x^2 + J_y^2)^{1/2}]$ spatial patterns for $V_0 = -0.5$, $D = 6$, and $M = 25$. $T = 50D$ is the time that the KH vortex starts to roll up. At $T = 70D$ during the rolling-up phase, the current density is enhanced at the hyperbolic point where the flow from above and below

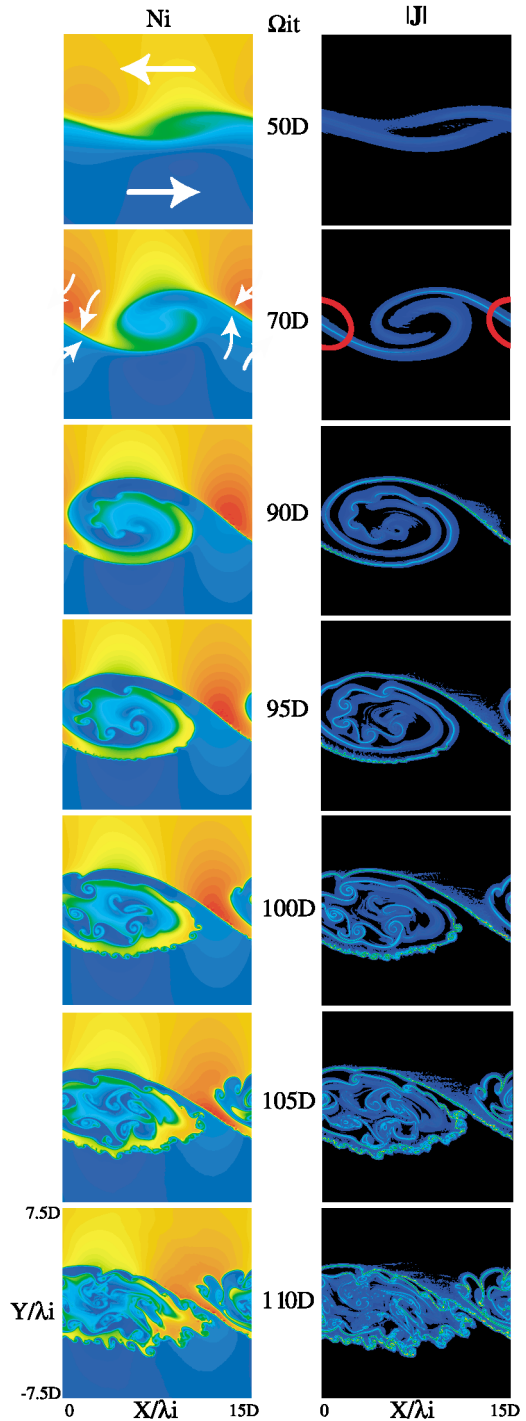


FIG. 1 (color). Time sequence of the density (left) and the current density (right) patterns depicting decay of a MHD-scale vortex by parasitic electron dynamics.

converge. At $T = 90D$, within the parent vortex, smaller vortices whose wavelengths are about a quarter of the parent's are emerging. The smaller vortices grow as time elapses, and finally at $T = 110D$ they begin to destroy the well-ordered pattern of the parent vortex. Such a quick decay of the vortex is not observed when the electron inertia is turned off (Hall-MHD), indicating that the electron inertial effects are crucial.

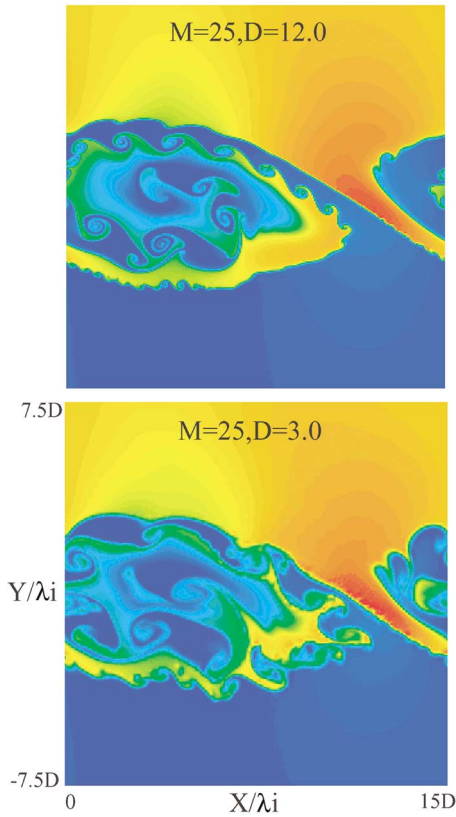


FIG. 2 (color). Dependence of the vortex decay process on the initial thickness of the velocity shear layer D . Density pattern at $T = 100D$ for $D = 3$ and 12 are shown ($M = 25$).

To find how the ratio D/λ_{e0} affects the decay process, we have made runs with various initial thickness D while keeping the mass ratio $M = 25$. Figure 2 shows the density pattern at $T = 100D$ for $D = 3$ and 12 , respectively. While D is varied by a factor of 4, emergence of smaller vortices whose wavelengths are $\sim 1/4$ of the parent's stays the same. In other words, the decay process is rather insensitive to the spatial scale ratio.

The above question can be readdressed by changing the mass ratio M . Figure 3 shows the results at $T = 100D$ for $M = 1600$ and $D = 1.5$. Again, despite the factor of 4 difference in the spatial scale ratio [$D/\lambda_{e0} = 15$ in Fig. 2 versus 60 in Fig. 3], the essential dynamics leading to the quick vortex decay is unchanged.

The decay process requires electron inertial effects but is insensitive to the spatial scale ratio. We propose the following scenario for this puzzling feature [20]: (i) The seed perturbations for the smaller vortices are produced by the current sheet kink instability (CSKI) [21] at the hyperbolic point where the current sheet is highly pinched during the rolling-up phase ($T = 70D$). The instability requires finite mass of electrons. (ii) This seed perturbation at the hyperbolic point propagates with the electron flow. When the sense of the shear is dusksidelike ($V_0 < 0$), the perturbation is brought to the secondary shear layer that develops at the outer edge of the parent vortex. (iii) The secondary shear is located at the density

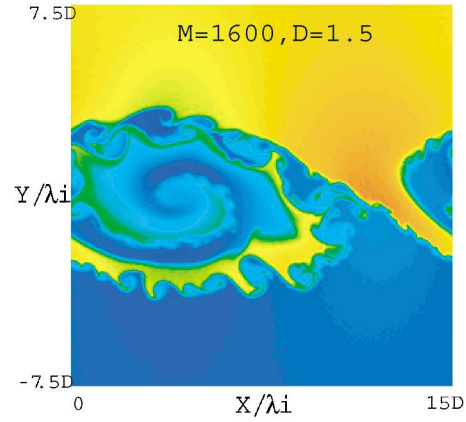


FIG. 3 (color). Dependence of the vortex decay process on the mass ratio M .

gradient layer and is present because the inner denser part rotates slower than the outer tenuous part under the same centrifugal force. The secondary shear layer thickness is $\sim \frac{1}{4}D$. (iv) The secondary shear is unstable to KHI whose wavelength is always about a quarter of the parent's ($\lambda_{2nd\ KH} \sim \frac{1}{4} \cdot 15D$).

Regarding (i), CSKI [21] is an instability that grows in thin current sheets. CSKI at the hyperbolic point and its propagation along the vortex outer edge are shown in Fig. 4. Shown is the color contour of J_y obtained at $T = 70D$ and $90D$ ($M = 25$ and $D = 3$). CSKI emerging at the hyperbolic point at $T = 70D$ is manifested as periodic variations of J_y . Its propagation along the vortex outer edge is evident at $T = 90D$. This parasitic CSKI produces perturbations of the wavelength $\lambda_{CSKI} \sim 6M^{-1/4}$, which varies with the mass ratio and is larger than λ_{e0} , but is smaller than $\lambda_{2nd\ KH}$. If not coupled to the secondary KHI, CSKI alone would not have triggered the decay process that remains viable in a thick shear layer. On the other hand, $\lambda_{2nd\ KH}$ increases with D while λ_{CSKI} stays the same. At huge D , vastly different wavelengths may reduce the coupling efficiency between the two modes. This would be the key issue in considering an astrophysical application, which is done later.

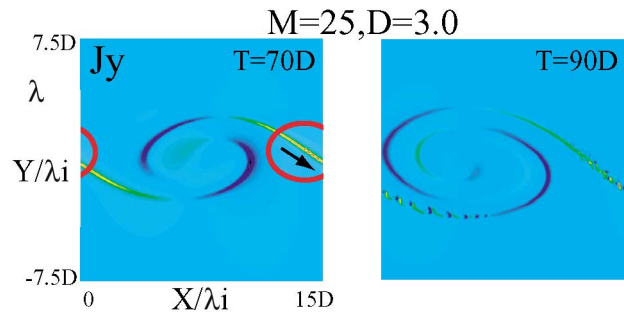


FIG. 4 (color). Color contours of J_y depicting excitation of CSKI at the hyperbolic point ($T = 70D$) and its propagation along the outer edge of the parent vortex ($T = 90D$).

Regarding (ii), when the sense of shear is reversed, the smaller vortices do not appear and thus the decay process is eliminated. In this case, CSKI at the hyperbolic point is still activated but the disturbances propagate with the electron flow in the opposite direction so as not to reach the secondary shear layer. The disturbances cause only unimpressive rippling of the current layer.

Regarding (iii), while it is one of the key issues of the decay process, we have not understood what makes the secondary shear layer thickness to be always $\sim \frac{1}{4}D$. The secondary shear is stronger with larger density ratio R , and we have confirmed that the secondary KHI grows fast enough for the quick vortex decay as long as $R > 1.5$.

Regarding (iv), the secondary KHI itself is an MHD process so that it should emerge even without electron inertial effects as long as there is appropriate seeding. In a numerical experiment by a Hall-MHD code, we added velocity fluctuations similar to those produced by CSKI at the hyperbolic point when the parent vortex is rolling up ($T = 70D$). Subsequently, smaller vortices excited by the secondary KHI appeared and the decay process was induced. As such, the role of the electron inertia is to naturally seed the secondary KHI in the right place at the right time for the quick decay.

An independent confirmation of the above statements has been done by various numerical experiments in which we have turned on/off the electron inertial effects during the runs. The key conclusion is that the vortex decay is available as long as the electron inertial effect is on between $T = 50D$ and $70D$. That is, the electron effect is needed when the parent vortex is starting to roll up but not necessarily when the decay itself is in progress.

While we have shown that the electron inertial effect is capable of inducing the decay, some other non-MHD effects not included here may well dominate in some situations. The present results should be regarded as the first demonstration that shows coupling to non-MHD dynamics within an MHD-scale vortex can change the MHD-scale behavior of it.

Decay of a large scale vortex may lead to large scale mixing of plasmas that used to be on different sides of a shear layer. Such mixing is taking place in the magnetotail boundary [22]. While the mixing of shocked-solar wind and magnetospheric plasmas are seen occasionally in the boundary layer on both dawn and dusk sides, the duskside mixing often shows a peculiar feature in which two populations remain separated in the velocity space [23–25]. Such a “collisionless” mixing may be achieved by the vortex decay, which is indeed expected on duskside.

Let us see if the vortex decay is possible in the tail boundary situation. The density ratio across the boundary R is 5–10 so that quick growth of the secondary KHI is well expected as long as there is appropriate seeding. The largest wavelength ratio $\lambda_{2nd\ KH}/\lambda_{CSKI}$ among the cases we have inspected is for the $M = 25$ and $D = 12$ case. At the real mass ratio, this wavelength ratio corresponds to

the $D = 4\text{--}5$ situation. Our results from the realistic mass ratio cases ($M = 1600$, $D = 1$, and 1.5) show that CSKI at the hyperbolic point is activated when the current density exceeds 0.6. Our high resolution Hall-MHD run for $D = 4$ shows that the current density does exceed 0.6 during the vortex roll-up phase ($T \sim 60D$). From these, we can expect excitation of CSKI and its coupling to the secondary KHI for the $D = 4\text{--}5$ and $M = 1836$ case, which reasonably models the tail boundary situation. It is concluded that the quick vortex decay is quite possible in the duskside tail boundary layer.

-
- [1] A. Miura, Phys. Rev. Lett. **49**, 779 (1982).
 - [2] J. U. Brackbill and D. A. Knoll, Phys. Rev. Lett. **86**, 2329 (2001).
 - [3] D. A. Knoll and L. Chacon, Phys. Rev. Lett. **88**, 215003 (2002).
 - [4] P. Comte, M. Lesieur, and E. Lamballais, Phys. Fluids A **4**, 2761 (1992).
 - [5] P. Comte, J. H. Silvestrini, and P. Begou, Eur. J. Mech. B **17**, 615 (1998).
 - [6] J. A. Wesson, Nucl. Fusion **30**, 2545 (1990).
 - [7] M. Ottaviani and F. Porcelli, Phys. Rev. Lett. **71**, 3802 (1993).
 - [8] J. Birn *et al.*, J. Geophys. Res. **103**, 3715 (2001).
 - [9] D. Del Sarto, F. Califano, and F. Pegoraro, Phys. Rev. Lett. **91**, 235001 (2003).
 - [10] M. Fujimoto, T. Tonooka, and T. Mukai, in *Earth's Low-Latitude Boundary Layer* (American Geophysical Union, Washington, DC, 2003).
 - [11] M. Fujimoto and T. Terasawa, J. Geophys. Res. **99**, 8601 (1994).
 - [12] W. Lennartsson and E. G. Shelley, J. Geophys. Res. **91**, 3061 (1986).
 - [13] D. G. Mitchell *et al.*, J. Geophys. Res. **92**, 7394 (1987).
 - [14] S. Wing and P. T. Newell, Geophys. Res. Lett. **29**, 10.1029/2001GL013950 (2002).
 - [15] M. Fujimoto and T. Terasawa, J. Geophys. Res. **100**, 12025 (1995).
 - [16] M. Wilber and R. M. Winglee, J. Geophys. Res. **100**, 1883 (1995).
 - [17] D. Biskamp, *Magnetic Reconnection in Plasmas* (Cambridge University Press, Cambridge, England, 2000).
 - [18] A. Miura and P. L. Pritchett, J. Geophys. Res. **87**, 7431 (1982).
 - [19] I. Shinohara (to be published).
 - [20] T. K. M. Nakamura and M. Fujimoto, in “Frontiers in Magnetospheric Physics” (Elsevier, Oxford, to be published).
 - [21] H. Suzuki, M. Fujimoto, and I. Shinohara, Adv. Space Res. **30/12**, 2663 (2002).
 - [22] M. Fujimoto, T. Terasawa, and T. Mukai, in *New Perspective on Earth's Magnetotail* (American Geophysical Union, Washington, DC, 1998).
 - [23] M. Fujimoto *et al.*, J. Geophys. Res. **103**, 4391 (1998).
 - [24] T. Phan *et al.*, J. Geophys. Res. **105**, 5497 (2000).
 - [25] H. Hasegawa *et al.*, J. Geophys. Res. **108**, 10.1029/2002JA009667 (2003).